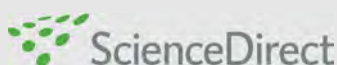
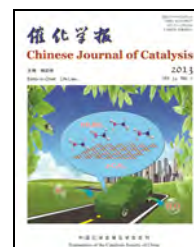




available at www.sciencedirect.com



journal homepage: www.elsevier.com/locate/chnjc



Article

Synthesis, characterization, and catalytic performance of bifunctional titanium silicalite-1

LI Hao^{a,b}, LEI Qian^a, ZHANG Xiaoming^{a,*}, SUO Jishuan^a

^a Chengdu Institute of Organic Chemistry, Chinese Academy of Sciences, Chengdu 610041, Sichuan, China

^b College of Chemistry and Environmental Engineering, Yangtze University, Jingzhou 434023, Hubei, China

ARTICLE INFO

Article history:

Received 31 January 2013

Accepted 27 March 2013

Published 20 July 2013

Keywords:

Titanium silicalite-1

Aluminium

Boron

Iron

Bifunctional catalyst

Ethylene

Selective oxidation

ABSTRACT

A series of bifunctional Ti-molecular sieves (M-TS-1, M = Al, B, or Fe) containing different trivalent ions (Al^{3+} , B^{3+} , or Fe^{3+}), with MFI topology, were synthesized using tetrapropylammonium bromide, silica sol, and *n*-butylamine as a template, base, and Si source, respectively. The simultaneous presence of Ti and trivalent ions in lattice positions provided catalysts with activity in both oxidation and acid-catalyzed reactions. The samples were characterized using X-ray diffraction, Fourier-transform infrared spectroscopy, ultraviolet-visible spectroscopy, NH_3 temperature-programmed desorption, inductively coupled plasma atomic emission spectroscopy, and N_2 adsorption-desorption isotherms. The results showed that the numbers and strength of acid sites of TS-1 were enhanced by the incorporation of trivalent ions. Using selective oxidation of ethylene as the probe reaction, the catalytic properties of M-TS-1 were investigated. The results showed that Al-TS-1 and B-TS-1 had better catalytic properties; conversion and utilization of H_2O_2 reached 95% and 90%, respectively, and the yield of ethylene glycol plus its monomethyl ether was greater than 10%.

© 2013, Dalian Institute of Chemical Physics, Chinese Academy of Sciences.
Published by Elsevier B.V. All rights reserved.

1. Introduction

Titanium silicalite-1 (TS-1) was first synthesized by Tamasso et al. [1] in 1983 and received extensive attention because it shows excellent performance in selective oxidation reactions with dilute H_2O_2 as the oxidant, requires mild reaction conditions, has high activity and selectivity, and is environmentally benign [2–4]. Recently, several studies of the synthesis of zeolites containing both Ti and a trivalent element (Al^{3+} , Ga^{3+} , Fe^{3+} , or B^{3+}) in MFI structure have been reported [5–14]. The simultaneous presence of Ti and trivalent elements in lattice positions provides catalysts that are active in both oxidation and acid-catalyzed reactions. One class of methods for the preparation of bifunctional Ti silicalite-1 (M-TS-1) [5–10] is based on hydrothermal crystallization of a hydrogel

obtained by basic hydrolysis of the respective precursors with aqueous tetrapropylammonium hydroxide (TPAOH). Bellussi et al. [5] have synthesized Al-TS-1, Ga-TS-1, and Fe-TS-1 using hydrothermal synthesis. The resulting materials exhibited high activity in the epoxidation of 1-butene, hydroxylation of phenol, and oligomerization of 1-octene, indicating that the acidity of the zeolite is enhanced by the incorporation of trivalent ions. Trong On et al. [6,9] have synthesized B-TS-1 by in-situ incorporation of B^{3+} and Ti^{4+} ions into the MFI structure during hydrothermal synthesis. The bifunctional catalyst effectively catalyzes the epoxidation of 1-hexene and 1-octene, followed by ring opening of the epoxide through hydrolysis and solvolysis reactions. Another class of methods for M-TS-1 preparation [11–14] is based on wetness impregnation of amorphous $\text{M}_2\text{O}_3\text{-TiO}_2\text{-SiO}_2$ (M = Al or Fe) solids with TPAOH solution and

* Corresponding author. Tel: +86-28-85226215; Fax: +86-28-85223978; E-mail: xm.zhang@cioc.ac.cn

DOI: 10.1016/S1872-2067(12)60589-0 | http://www.sciencedirect.com/science/journal/18722067 | Chin. J. Catal., Vol. 34, No. 7, July 2013

subsequent crystallization under autogenous pressure. Ovejero et al. [13] synthesized Al-TS-1 by wetness impregnation of amorphous $\text{Al}_2\text{O}_3\text{-TiO}_2\text{-SiO}_2$ solids. Al-TS-1 showed high activity for *n*-hexane oxidation and methanol/*tert*-butyl alcohol etherification, suggesting that the catalyst is active in both oxidation and acid-catalyzed reactions. However, the two classes of methods for M-TS-1 preparation mentioned above use expensive TPAOH as the template, and the synthesis requires stringent conditions (alkali-free TPAOH solutions).

Recently, we successfully prepared Al-TS-1 using tetrapropylammonium bromide (TPABr), silica sol, and *n*-butylamine (NBA) as a template, silica source, and base, respectively [15]. Both the number of acid sites in TS-1 and the site acidity were enhanced by the incorporation of Al^{3+} . Al-TS-1 exhibited high catalytic activity in the selective oxidation of ethylene to ethylene glycol (EG) using a mixed solvent consisting of methanol and water. In this work, the synthesis, characterization, and catalytic properties of M-TS-1 (M = Al, B, or Fe) in the selective oxidation of ethylene were further studied.

2. Experimental

2.1. Preparation of M-TS-1

M-TS-1 was prepared using a previously reported method [15] from colloidal silica (30%, Qingdao Hengshengda Chemical Co., Ltd), tetrabutyl orthotitanate (TBOT, AR, Chengdu Kelong Chemical Reagent Factory), $\text{Al}(\text{NO}_3)_3\cdot 9\text{H}_2\text{O}$ (99.0%, Guangdong Guanghua Chemical Factory Co., Ltd), H_3BO_3 (99.5%, Shantou Guanghua Chemical Factory), and $\text{Fe}(\text{NO}_3)_3\cdot 9\text{H}_2\text{O}$ (98.5%, Guangdong Guanghua Chemical Factory Co., Ltd) as the sources of Si, Ti, Al, B, and Fe respectively. TPABr (99.0%, Jintan Southwest Chemical Institute) was used as the template, and NBA (AR, Chengdu Kelong Chemical Reagent Factory) was used as the base.

2.1.1. B-TS-1

In a typical synthesis, 12.8 g of TPABr and 92.7 g of silica sol (30%) were dissolved in 142 g of deionized water; the resulting mixture was denoted by solution 1. Also, 4.61 g of TBOT were dissolved in 6.4 g of aqueous H_2O_2 solution (30%), and 20.7 g of NBA were added (solution 2). Then solution 2 was slowly added to solution 1 under vigorous stirring, followed by dropwise addition of 0.082 g of H_3BO_3 dissolved in 50 g of deionized water. The molar composition was $\text{SiO}_2\text{:xB}_2\text{O}_3\text{:0.03TiO}_2\text{:0.6NBA:0.1TPABr:30H}_2\text{O}$, where $1/x = 200\text{--}800$. Finally, 1.2 g of TS-1 powder were added as seeds. After stirring at 333 K for 2 h to accelerate hydrolysis and evaporate the alcohol, the gel was transferred to a Teflon-lined autoclave and heated at 448 K under autogenous pressure for 72 h. Finally, the solid product was recovered by centrifugation, washed with distilled water, dried overnight at 373 K, and calcined at 823 K for 5 h. A reference TS-1 zeolite was also prepared using the synthesis procedure described above but omitting the H_3BO_3 addition step.

2.1.2. Fe-TS-1

The Fe-TS-1 molecular sieve was synthesized using a gel

with composition $\text{SiO}_2\text{:xFe}_2\text{O}_3\text{:0.03TiO}_2\text{:0.6NBA:0.1TPABr:30H}_2\text{O}$, where $1/x = 300\text{--}1000$. A typical preparation was similar to that of B-TS-1, the only difference being that a solution containing 0.519 g of $\text{Fe}(\text{NO}_3)_3\cdot 9\text{H}_2\text{O}$ in 50 g of deionized water instead of H_3BO_3 solution was added dropwise after addition of solution 2 to solution 1.

2.1.3. Al-TS-1

The Al-TS-1 catalyst was synthesized using a gel with composition $\text{SiO}_2\text{:0.002Al}_2\text{O}_3\text{:0.03TiO}_2\text{:0.6NBA:0.1TPABr:30H}_2\text{O}$. The preparation was similar to that of B-TS-1, the only difference being that a solution of 0.689 g of $\text{Al}(\text{NO}_3)_3\cdot 9\text{H}_2\text{O}$ in 50 g of deionized water instead of H_3BO_3 solution was added dropwise to solution 1 before solution 2 was added.

2.2. Characterization of M-TS-1

The samples were characterized using X-ray diffraction (XRD; Philips X'PERT, Cu K_α radiation), Fourier-transform infrared (FT-IR) spectroscopy (Nicolet MX-1E 560, KBr pellet technique), and ultraviolet-visible (UV-Vis) spectroscopy (TU-1091 spectrometer, BaSO_4 as reference). The chemical compositions of the samples were determined using inductively coupled plasma atomic emission spectroscopy (ICP-AES; Perkin-Elmer Optima DV 2000). Nitrogen adsorption-desorption isotherms were obtained on a Micromeritics ASAP 2420 instrument. Samples were degassed at 473 K under vacuum overnight prior to the measurements. NH_3 temperature-programmed desorption (NH_3 -TPD) measurements were performed in a fixed-bed reactor connected to a thermal conductivity detector (GC 2000II). The sample (about 100 mg) was initially activated at 673 K for 1 h in an ultrahigh-purity Ar flow (25 ml/min). It was then cooled to 373 K and pure NH_3 (20 ml/min) was adsorbed for 1.5 h. The sample was then flushed with pure Ar (25 ml/min) for 1 h at 373 K. The NH_3 -TPD curves of the samples were obtained by increasing the temperature from 373 to 873 K at a ramp rate of 10 K/min under a pure Ar flow of 25 ml/min.

2.3. Catalysis tests for selective oxidation of ethylene

The selective oxidation of ethylene with dilute H_2O_2 was carried out at 333 K in a stainless-steel autoclave reactor. In a typical run, 4.0 g of calcined catalyst, 40.0 ml of about 30% H_2O_2 , 50 ml of water, and 150 ml of methanol were fed into the stainless-steel autoclave reactor. Then ethylene was charged at a constant pressure (0.7 MPa). After heating the mixture at 333 K under agitation for a certain period, the residual H_2O_2 was checked by iodometric titration. The reaction products were analyzed using a gas chromatograph (Shanghai Techcomp Instrument Co., Ltd, GC 7890F chromatograph, SE-54, capillary column 15 m \times 0.25 mm) equipped with a flame ionization detector using acetonitrile as the internal standard. The GC analysis conditions were as follows: the column box temperature was 343 K, the gasification chamber temperature was 493 K, and the detector temperature was 493 K. EG and its monomethyl ether (MME) were the main products. The reac-

tion results are reported using the following criteria:

$$X(\text{H}_2\text{O}_2) = [n_0(\text{H}_2\text{O}_2) - n(\text{H}_2\text{O}_2)]/n_0(\text{H}_2\text{O}_2) \times 100\%$$

$$U(\text{H}_2\text{O}_2) = [n(\text{EG}) + n(\text{MME})]/[n_0(\text{H}_2\text{O}_2) \times X(\text{H}_2\text{O}_2)] \times 100\%$$

$$S(\text{EG}) = n(\text{EG})/[n(\text{EG}) + n(\text{MME})] \times 100\%$$

$$S(\text{MME}) = n(\text{MME})/[n(\text{EG}) + n(\text{MME})] \times 100\%$$

where $X(\text{H}_2\text{O}_2)$, $U(\text{H}_2\text{O}_2)$, $S(\text{EG})$, and $S(\text{MME})$ are the H_2O_2 conversion, the utilization of H_2O_2 , the selectivity for EG, and the selectivity for MME, respectively. The moles of EG and MME are represented by $n(\text{EG})$ and $n(\text{MME})$, respectively; $n_0(\text{H}_2\text{O}_2)$ and $n(\text{H}_2\text{O}_2)$ are the initial and final molar contents of H_2O_2 , respectively.

3. Results and discussion

3.1. Characterization results of M-TS-1

Table 1 lists the physicochemical properties of the TS-1 and M-TS-1 catalysts. The TS-1 contains a trace amount of Al from the silica sol used as the silicon source. Both Al and Ti were incorporated into the TS-1 framework [16,17]. The trivalent elements and Ti contents of the TS-1 and M-TS-1 are lower than those of the initial gel, indicating that not all the Al^{3+} , B^{3+} , Fe^{3+} , and Ti^{4+} are involved in the crystallization process [5,7,11]. The Brunauer-Emmett-Teller (BET) surface areas and micropore volumes of the TS-1 zeolite change little upon incorporation of trivalent ions, indicating that the pore structure is well preserved.

Figure 1 shows the XRD patterns of the TS-1 and M-TS-1. The samples show the characteristics of MFI topology without an impure phase, indicating that the incorporation of trivalent elements does not destroy the zeolite structure.

Table 1

Physicochemical properties of TS-1 and M-TS-1 zeolites.

Sample	Gel		Zeolite		A_{BET} (m^2/g)	$V_{\text{micropore}}$ (cm^3/g)	NH_3 (mmol/g)
	Si/Ti	Si/M	Si/Ti	Si/M			
TS-1	33.3	∞	36.5	393.1	399.0	0.11	0.13
Al-TS-1	33.3	252.0	42.1	434.5	395.9	0.11	0.21
B-TS-1	33.3	350.0	50.9	364.0	389.1	0.11	0.17
Fe-TS-1	33.3	360.0	51.1	375.4	390.3	0.11	0.19

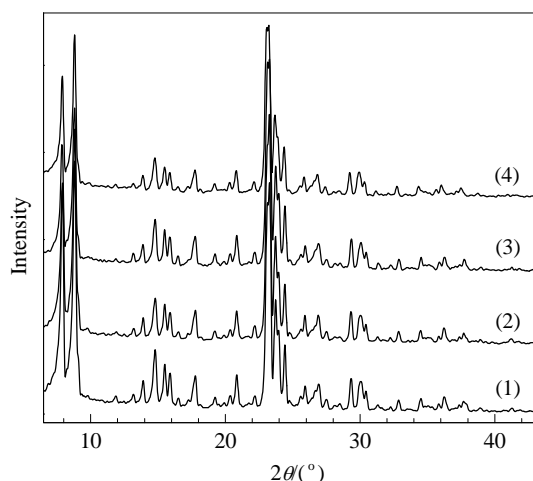


Fig. 1. XRD patterns of TS-1 and M-TS-1. (1) TS-1; (2) Al-TS-1 (Si/Al = 252); (3) B-TS-1 (Si/B = 350); (4) Fe-TS-1 (Si/Fe = 360).

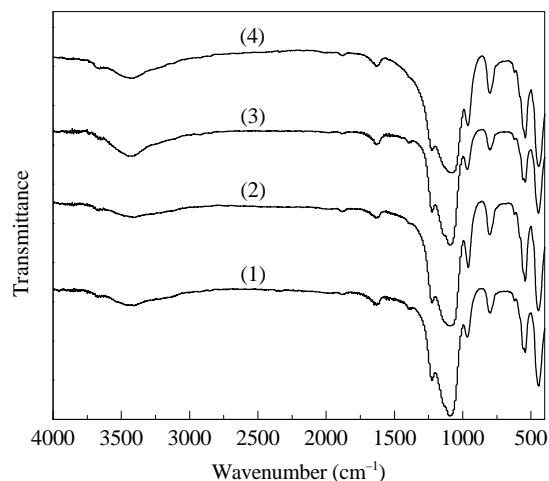


Fig. 2. FT-IR spectra of TS-1 and M-TS-1. (1) TS-1; (2) Al-TS-1 (Si/Al = 252); (3) B-TS-1 (Si/B = 350); (4) Fe-TS-1 (Si/Fe = 360).

Figure 2 shows FT-IR spectra of TS-1 and M-TS-1. The samples show a characteristic peak at about 960 cm^{-1} , attributed to the Si-O vibration in the $\text{O}_3\text{Si-O-Ti}$ structure, which indicates that Ti was incorporated into the zeolite framework [18].

Figure 3 shows the UV-Vis spectra of TS-1 and M-TS-1. The samples exhibit a main absorption band at about 220 nm , attributed to isolated Ti(IV) species, and another band at $270\text{--}280\text{ nm}$, attributed to Ti^{4+} ions octahedrally coordinated with two H_2O molecules in the coordination sphere, or small hydrated oligomeric TiO_x species [19]. There is also a weak peak at about 330 nm from extra-framework Ti oxide [20], indicating that some extra-framework Ti species are systematically generated in the presence of trivalent ions [7]. These results are in good agreement with the ICP-AES analysis (Table 1).

The acidity of the TS-1 and M-TS-1 catalysts was studied using NH_3 -TPD, and the profiles are shown in Fig. 4. An NH_3 desorption peak at about 444.1 K was observed for TS-1, and its NH_3 adsorption capacity was $0.13\text{ mmol}/\text{g}$ (Table 1), indicating that TS-1 prepared in this study had weak acid sites [16,17]. When additional trivalent ions (Al^{3+} , B^{3+} , or Fe^{3+}) were

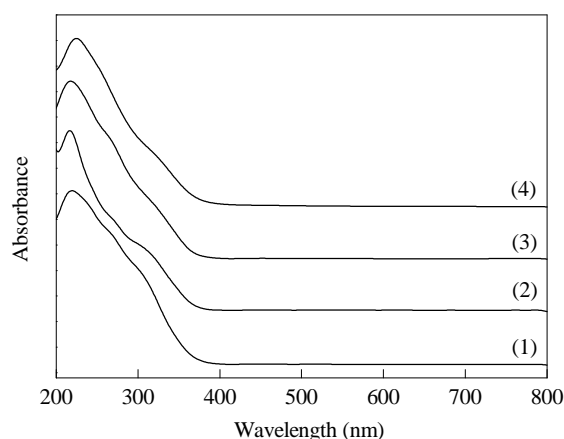


Fig. 3. UV-Vis spectra of TS-1 and M-TS-1. (1) TS-1; (2) Al-TS-1 (Si/Al = 252); (3) B-TS-1 (Si/B = 350); (4) Fe-TS-1 (Si/Fe = 360).

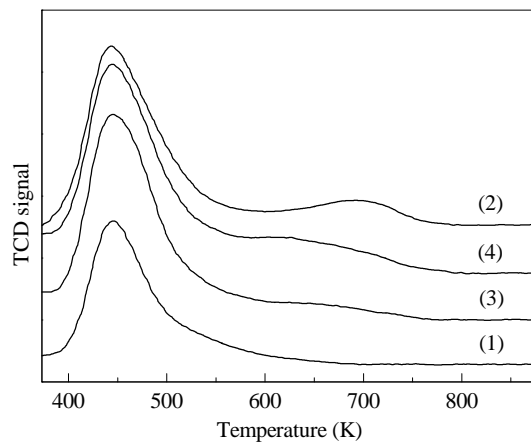


Fig. 4. NH_3 -TPD profiles of TS-1 and M-TS-1. (1) TS-1; (2) Al-TS-1 (Si/Al = 252); (3) B-TS-1 (Si/B = 350); (4) Fe-TS-1 (Si/Fe = 360).

introduced, the intensity of the peak at about 444.1 K increased significantly, and a small broad desorption peak (at 677.4 K for B-TS-1 and Fe-TS-1, and at 701.9 K for Al-TS-1) appeared. The order of the acid strengths was TS-1 < B-TS-1 < Fe-TS-1 < Al-TS-1 (Table 1), which is in consistent with the results for the FT-IR spectra of adsorbed pyridine [7]. These results indicated that the amounts and strength of the acid sites of TS-1 were both enhanced by introducing trivalent ions during preparation.

It is widely accepted that substitution by trivalent ions such

as Al^{3+} and B^{3+} or transition-metal ions such as Fe^{3+} can occur in many minerals. In contrast to most silicates, isomorphous substitution in a zeolite can only take place at tetrahedral sites [6]. It was reported that most of the trivalent ions (Al^{3+} , B^{3+} , and Fe^{3+}) were essentially incorporated into the TS-1 framework in tetrahedral environments [5,7–13].

3.2. Catalytic properties of M-TS-1

Figure 5(a) shows the results of selective oxidation of ethylene with dilute H_2O_2 over B-TS-1 with different B contents. When the $\text{SiO}_2/\text{B}_2\text{O}_3$ molar ratio decreased from 800 to 700, the H_2O_2 conversion and EG and MME selectivity changed little, but the H_2O_2 utilization and the yield of EG plus MME increased significantly. When the $\text{SiO}_2/\text{B}_2\text{O}_3$ molar ratio decreased from 700 to 500, the H_2O_2 conversion and EG and MME selectivity changed little, and the H_2O_2 utilization and the yield of EG plus MME decreased slightly. On further decreasing the $\text{SiO}_2/\text{B}_2\text{O}_3$ to 200, the H_2O_2 conversion and EG and MME selectivity changed little, but the H_2O_2 utilization and the yield of EG plus MME decreased significantly. These results indicate that when an excess of B is introduced, the degree of H_2O_2 decomposition is enhanced [8,9]. B-TS-1 ($\text{SiO}_2/\text{B}_2\text{O}_3 = 350$) should therefore be an appropriate catalyst.

Figure 5(b) shows the results of selective oxidation of ethylene with dilute H_2O_2 over Fe-TS-1 with different Fe contents. When the $\text{SiO}_2/\text{Fe}_2\text{O}_3$ molar ratio decreased from 1000 to 720, the H_2O_2 conversion and EG and MME selectivity changed little,

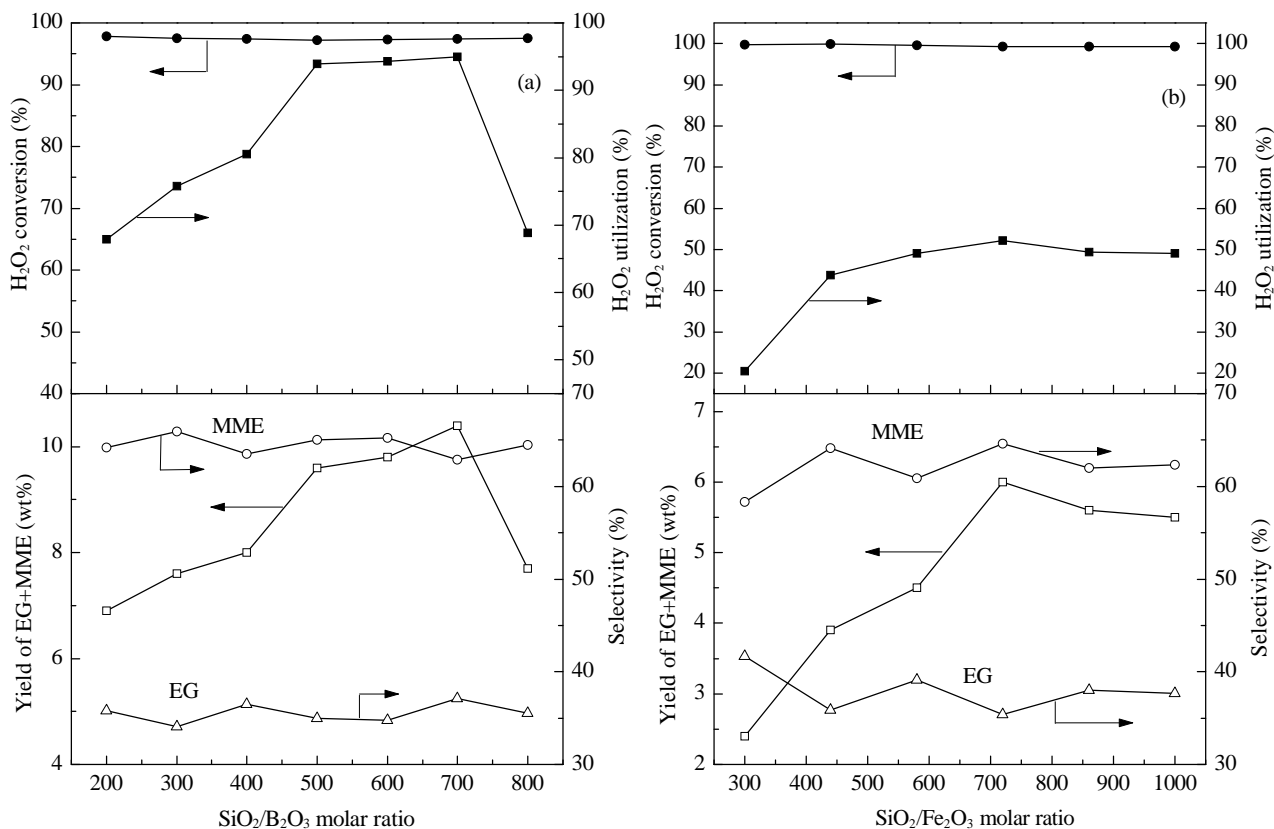


Fig. 5. Selective oxidation of ethylene with dilute H_2O_2 over B-TS-1 with different B contents (a) and over Fe-TS-1 with different Fe contents (b). Reaction conditions: ethylene pressure 0.7 MPa, H_2O_2 1.7 mol/L, catalyst 17.2 g/L, methanol/water (molar ratio 0.8) mixed solvent, 333 K, 8 h.

but the H_2O_2 utilization and the yield of EG plus MME increased significantly. On further decreasing the $\text{SiO}_2/\text{Fe}_2\text{O}_3$ molar ratio, the H_2O_2 conversion and EG and MME selectivity changed little, but the H_2O_2 utilization and yield of EG plus MME began to decrease. When the $\text{SiO}_2/\text{Fe}_2\text{O}_3$ was 720, Fe-TS-1 gave a relatively good catalytic performance.

In the selective oxidation of ethylene with dilute H_2O_2 over Al-TS-1 ($\text{Si}/\text{Al} = 252$) using the mixed solvent methanol and water, the conversion and utilization of H_2O_2 were 98.3% and 92.3%, respectively, and the yield of EG plus MME was 10.1%. Investigation of the catalytic performance of Al-TS-1 ($\text{Si}/\text{Al} = 252$) and B-TS-1 ($\text{Si}/\text{B} = 350$) showed that they had high catalytic activity and selectivity. The conversion and utilization of H_2O_2 reached 95% and 90%, respectively, and the yield of EG plus MME was above 10%. However, Fe-TS-1 ($\text{Si}/\text{Fe} = 360$) exhibited poor catalytic selectivity because of its strong ability to decompose H_2O_2 [5].

3.3. Reaction mechanism

To study the relation between H_2O_2 decomposition and selective oxidation of ethylene, a blank experiment was conducted. The conversion of H_2O_2 was 14.6%, and H_2O_2 utilization and the yield of EG plus MME were zero. Comparing the results of the blank experiment with those using M-TS-1, it could be concluded that H_2O_2 decomposition and selective oxidation of ethylene are competing reactions. In the cases of Al-TS-1 and B-TS-1, the effect of trivalent ions on H_2O_2 decomposition could

be neglected, but this was not consistent with results reported in the literature [5,8,9].

Figure 6(a) shows the effect of reaction time on the selective oxidation of ethylene over Al-TS-1. It can be seen that the yield of EG plus MME and the conversion and utilization of H_2O_2 increased linearly with increasing reaction time (from 1 to 4 h). On further prolonging the reaction time, the yield of EG plus MME and the conversion and utilization of H_2O_2 changed little. The selectivity for MME and EG remained constant with increasing reaction time (Fig. 6(a)). Moreover, one can clearly see that the MME selectivity was about twice that for EG for all reaction time. An appropriate reaction time was therefore 4 h.

Figure 6(b) shows the effect of reaction time on the selective oxidation of ethylene over B-TS-1. On prolonging the reaction time from 1 to 4 h, the yield of EG plus MME and the conversion and utilization of H_2O_2 increased linearly. When the reaction time was increased to 7 h, the yield of EG plus MME and the conversion and utilization of H_2O_2 increased slightly. When the reaction time was prolonged further, the H_2O_2 conversion changed little, but H_2O_2 utilization and the yield of EG plus MME began to decrease. The selectivity for MME and EG was constant for all reaction time (Fig. 6(b)). Moreover, one can clearly see that the MME selectivity was about twice that for EG for all reaction time; this was similar to the case for Al-TS-1. The appropriate reaction time was therefore 7 h, which is longer than that for Al-TS-1. The discrepancy between the optimum reaction time might be caused by the different physicochemical properties of the trivalent ions [7].

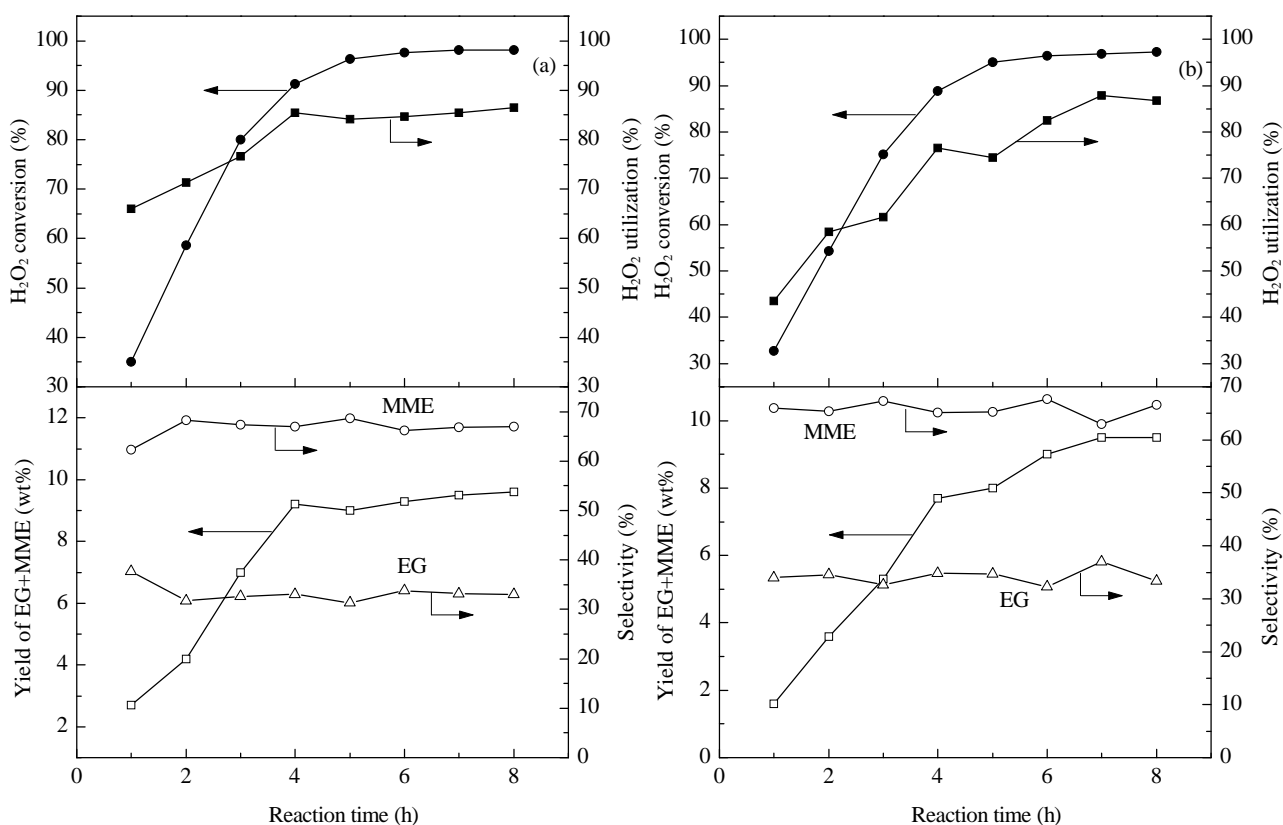
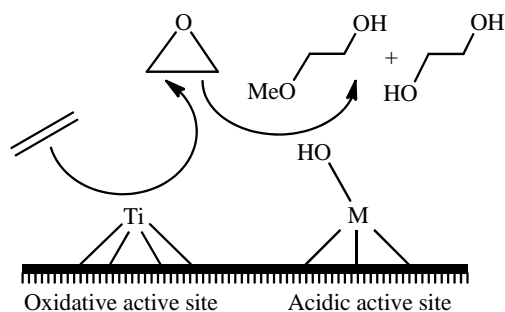


Fig. 6. Effect of reaction time on selective oxidation of ethylene over Al-TS-1 ($\text{Si}/\text{Al} = 252$) (a) and B-TS-1 ($\text{Si}/\text{B} = 350$) (b). Reaction conditions were the same as those in Fig. 5.



Scheme 1. Proposed model of M-TS-1 (M = Al or B) as a bifunctional catalyst for ethylene epoxidation and subsequent ring-opening process.

In the ethylene epoxidation and subsequent ring-opening process, if the hydrolysis and methanolysis of ethylene epoxide are slow reactions, then oxirane would be one of the final products; however, we did not detect oxirane using GC. The solvolysis of oxirane was therefore fast, and the ethylene epoxidation step was the slow and rate-determining step. As a result of the hydrophobic character of TS-1, methanol approaches Ti sites more readily than water does, leading to the formation of more stable five-membered-ring intermediates [21]. In addition, because of the stronger nucleophilicity of the alcohol compared with water [22], methanolysis of oxirane was easier than hydrolysis. The MME selectivity was therefore higher than that for EG for all reaction time. Because the epoxide immediately reacted with active acid sites in M (Al or B) to solvolyze oxirane, the trivalent ions (Al^{3+} or B^{3+}) incorporated into the framework of TS-1 would effectively be located close to Ti active sites. On the basis of these results, a model of the bifunctional oxidative and acidic catalytic system for consecutive reactions of ethylene to MME and EG is proposed and is shown in Scheme 1 [15].

4. Conclusions

M-TS-1 was prepared by introducing a trivalent ion into the TPABr-NBA system. M-TS-1 was active in both oxidation and acid-catalyzed reactions. Characterization using various techniques showed that trivalent ions were incorporated into the TS-1 framework, and the MFI structure was well preserved in M-TS-1. The introduction of trivalent ions into the framework

of the TS-1 zeolite resulted in increases in the numbers and strength of the acid sites; the order of the acid strength was $\text{TS-1} < \text{B-TS-1} < \text{Fe-TS-1} < \text{Al-TS-1}$. The oxidative and acid-catalyzed activity was adjusted by introducing different concentrations of trivalent elements into the zeolite framework. Al-TS-1 ($\text{Si/Al} = 252$) and B-TS-1 ($\text{Si/B} = 350$) exhibited higher catalytic activity in the selective oxidation of ethylene; the conversion and utilization of H_2O_2 reached 95% and 90%, respectively, and the yield of EG plus MME reached 10%. These values are comparable to those achieved in current industrial processes for EG production. Finally, a model of M-TS-1 as a bifunctional catalyst for ethylene epoxidation and a subsequent ring-opening process was proposed.

References

- [1] Taramasso M, Perego G, Notari B. US Patent 4 410 501. 1983
- [2] Ratnasamy P, Srinivas D, Knözinger H. *Adv Catal*, 2004, 48: 1
- [3] Yang J X, Yao M K, Zhao S, Liu Y M, Wu P, He M Y. *Chin J Catal* (杨俊霞, 姚明楷, 赵松, 刘月明, 吴鹏, 何鸣元. 催化学报), 2010, 31: 95
- [4] Deng X J, Shen L, Zhang Sh, Liu Y M. *Chin J Catal* (邓秀娟, 申璐, 张硕, 刘月明. 催化学报), 2011, 32: 1550
- [5] Bellusi G, Carati A, Clerici M G, Esposito A. *Stud Surf Sci Catal*, 1991, 63: 421
- [6] Trong On D, Kaliaguine S, Bonnevot L. *J Catal*, 1995, 157: 235
- [7] Trong On D, Nguyen S V, Hulea V, Dumitriu E, Kaliaguine S. *Microporous Mesoporous Mater*, 2003, 57: 169
- [8] Trong On D, Kapoor M P, Bonnevot L, Kaliaguine S, Gabelica Z. *J Chem Soc, Faraday Trans*, 1996, 92: 1031
- [9] Kapoor M P, Trong On D, Gallot J E, Kaliaguine S. *Catal Lett*, 1997, 43: 127
- [10] Pirutko L V, Uriarte A K, Chernyavsky V S, Kharitonov A S, Panov G I. *Microporous Mesoporous Mater*, 2001, 48: 345
- [11] Ovejero G, van Grieken R, Uguina M A, Serrano D P, Melero J A. *Catal Lett*, 1996, 41: 69
- [12] Melero J A, van Grieken R, Serrano D P, Espada J J. *J Mater Chem*, 2001, 11: 1519
- [13] Ovejero G, van Grieken R, Uguina M A, Serrano D P, Melero J A. *J Mater Chem*, 1998, 8: 2269
- [14] Ovejero G, Sotelo J L, Martínez F, Melero J A, Gordo L. *Ind Eng Chem Res*, 2001, 40: 3921
- [15] Li H, Lei Q, Zhang X M, Suo J S. *Catal Commun*, 2009, 10: 1936
- [16] Guo X W, Wang X S, Liu M, Li G, Chen Y Y, Xiu J H, Zhuang J Q, Zhang W P, Bao X H. *Catal Lett*, 2002, 81: 125

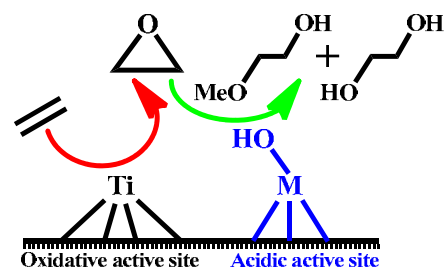
Graphical Abstract

Chin. J. Catal., 2013, 34: 1363–1372 doi: 10.1016/S1872-2067(12)60589-0

Synthesis, characterization, and catalytic performance of bifunctional titanium silicalite-1

Li Hao, LEI Qian, ZHANG Xiaoming*, SUO Jishuan
Chengdu Institute of Organic Chemistry, Chinese Academy of Sciences;
Yangtze University

The coinorporation of Ti and a trivalent ion into the MFI-type zeolite was studied. The acidity of TS-1 was enhanced by introducing trivalent ions. M-TS-1 showed higher activity in the selective oxidation of ethylene.



- [17] Li G, Wang X Sh, Yan H Sh, Liu M, Liu Y H, Chen Y Y. *Chin J Catal* (李钢, 王祥生, 闫海生, 刘民, 刘毅慧, 陈永英. 催化学报), 2001, 22: 465
- [18] Scarano D, Zecchina A, Bordiga S, Geobaldo F, Spoto G, Petrini G, Leofanti G, Padovan M, Tozzola G. *J Chem Soc, Faraday Trans*, 1993, 89: 4123
- [19] Wang X S, Guo X W, Li G. *Catal Today*, 2002, 74: 65
- [20] Boccuti M R, Rao K M, Zecchina A, Leofanti G, Petrini G. *Stud Surf Sci Catal*, 1989, 48: 133
- [21] Fan W B, Wu P, Tatsumi T. *J Catal*, 2008, 256: 62
- [22] Liu X Y, Yin D L, Zhu H Y, Shen G. *Chin J Catal* (刘绚艳, 尹笃林, 朱华元, 沈刚. 催化学报), 2010, 31: 72

双功能钛硅分子筛的合成、表征及催化性能

李 颢^{a,b}, 雷 骞^a, 张小明^{a,*}, 索继栓^a

^a中国科学院成都有机化学研究所, 四川成都610041

^b长江大学化学与环境工程学院, 湖北荆州434023

摘要: 以四丙基溴化铵为模板剂, 硅溶胶为硅源, 正丁胺为碱源, 采用水热合成的方法, 将三价离子(Al^{3+} , B^{3+} 或 Fe^{3+})和 Ti^{4+} 同时引入到MFI型分子筛的骨架, 得到同时具有氧化和酸催化活性的双功能钛硅分子筛M-TS-1 ($\text{M} = \text{Al}$, B 或 Fe)。通过X射线粉末衍射、傅里叶变换红外光谱、紫外-可见漫反射光谱、氨程序升温脱附、电感耦合等离子体原子发射光谱和 N_2 吸附-脱附等温线手段对样品进行了表征。结果表明, 三价离子的引入, 提高了TS-1的酸强度和酸量。采用乙烯选择氧化为探针反应考察了M-TS-1的催化性能。结果表明, Al-TS-1和B-TS-1在乙烯环氧化及后续的开环溶剂解反应中表现出较高的催化性能, H_2O_2 的转化率在95%以上, H_2O_2 的利用率大于90%, 乙二醇和乙二醇单甲醚的总收率可达10%以上。

关键词: 钛硅分子筛; 铝; 硼; 铁; 双功能催化剂; 乙烯; 选择氧化

收稿日期: 2013-01-31. 接受日期: 2013-03-27. 出版日期: 2013-07-20.

*通讯联系人. 电话: (028)85226215; 传真: (028)85223978; 电子信箱: xm.zhang@cioc.ac.cn

本文的英文电子版由Elsevier出版社在ScienceDirect上出版(<http://www.sciencedirect.com/science/journal/18722067>).

1. 前言

钛硅分子筛TS-1自Taramasso等^[1]首次报道合成以来, 由于其优异的选择氧化催化性能及其催化的反应具有对环境污染轻、反应条件温和等优点而备受关注^[2-4]。近年来, 研究者^[5-14]尝试在分子筛的合成过程中引入其它三价离子(Al^{3+} , Ga^{3+} , Fe^{3+} 或 B^{3+} 等)修饰其催化性能。 Ti^{4+} 和三价离子同时进入分子筛的骨架, 使分子筛不但对氧化反应有催化活性, 而且对酸催化反应也有催化活性。双功能钛硅分子筛的一类制备方法^[5-10]是利用原料在四丙基氢氧化铵(TPAOH)水溶液中分别水解, 制得水凝胶, 然后对该凝胶进行水热晶化。Bellussi等^[5]采用水热合成法制备了Al-TS-1, Ga-TS-1和Fe-TS-1, 它们在1-丁烯液相环氧化、苯酚羟基化和1-辛烯低聚反应中均表现出较好的催化活性, 说明三价金属的引入增加了TS-1分子筛的酸性。Trong On等^[6,9]采用水热合成法将 B^{3+} 和 Ti^{4+} 直接引入分子筛骨架, 合成出具有氧化和酸催化活性的B-TS-1, 其在1-己烯和1-辛烯的选择氧化反应中促进了环氧化物的开环水解和溶剂解。双功能钛硅分子筛的另一类制备方法^[11-14]是以非晶固体 $\text{M}_2\text{O}_3\text{-TiO}_2\text{-SiO}_2$ ($\text{M} = \text{Al}$ 或 Fe)为原料, 用TPAOH溶液浸渍, 然后水热晶化。Ovejero等^[13]以非晶的 $\text{Al}_2\text{O}_3\text{-TiO}_2\text{-SiO}_2$ 为原料, 通过浸渍法合成出Al-TS-1, 其在正己烷氧化和甲醇与叔丁

醇的醚化反应中均表现出较高的催化活性, 说明Al-TS-1同时具有氧化和酸催化性能。但是, 上述两类方法都需要采用价格昂贵的TPAOH为原料, 而且操作条件苛刻。

最近, 我们采用四丙基溴化铵(TPABr)为模板剂, 硅溶胶为硅源, 正丁胺为碱源, 成功地制备出Al-TS-1^[15]。 Al^{3+} 的引入增大了TS-1的酸强度和酸量。采用甲醇和水混合溶剂, Al-TS-1在乙烯选择氧化制乙二醇的反应中表现出良好的催化性能。本文进一步研究了双功能钛硅分子筛Al-TS-1, B-TS-1和Fe-TS-1的制备、表征及其在乙烯选择氧化反应中的催化性能。

2. 实验部分

2.1. 分子筛的合成

参照文献^[15]制备双功能钛硅分子筛M-TS-1。采用硅溶胶($w(\text{SiO}_2) = 30\%$, 青岛恒盛达化工有限公司)为硅源, 钛酸正丁酯(TBOT, 分析纯, 成都市科龙化工试剂厂)为钛源, 四丙基溴化铵(99.0%, 金坛市西南化工研究所)为模板剂, 正丁胺(NBA, 分析纯, 成都市科龙化工试剂厂)为碱源, 九水合硝酸铝(99.0%, 广东光华化学厂有限公司)为铝源, 硼酸(99.5%, 汕头市光华化学厂)为硼源, 九水合硝酸铁(98.5%, 广东光华化学厂有限公司)为铁源。

2.1.1. B-TS-1的合成

首先, 将12.8 g TPABr和92.7 g硅溶胶溶解于142 g去离子水中, 得到溶液1; 另外配制TBOT (4.61 g)的H₂O₂ (30%, 6.4 g)络合水溶液, 加入20.7 g NBA, 得到溶液2. 在剧烈搅拌下, 将溶液2加入到溶液1中, 然后滴加一定浓度的硼酸水溶液, 所得溶液的物料比为SiO₂:x B₂O₃:0.03TiO₂:0.6NBA:0.1TPABr:30H₂O, 其中 1/x = 200~800. 最后, 加入1.2 g TS-1晶种, 加热至333 K蒸醇, 转移入高压釜(聚四氟乙烯为衬里), 448 K下晶化3 d. 将得到的晶化产物过滤, 水洗至pH = 7, 在373 K下过夜干燥, 最后在马弗炉中823 K下焙烧5 h, 即得B-TS-1分子筛. 作为对照, 按照上述合成步骤制备TS-1分子筛, 只是不添加硼酸.

2.1.2. Fe-TS-1的合成

按照摩尔比配料 SiO₂:x Fe₂O₃:0.03TiO₂:0.6NBA:0.1TPABr:30H₂O (1/x = 300~1000)合成Fe-TS-1. 其合成操作与B-TS-1类似, 将一定浓度的硼酸水溶液换成一定浓度的硝酸铁水溶液即可.

2.1.3. Al-TS-1的合成

按照摩尔比配料 SiO₂:0.002Al₂O₃:0.03TiO₂:0.6NBA:0.1TPABr:30H₂O合成Al-TS-1. 其合成操作与B-TS-1类似, 只不过将一定浓度的硝酸铝水溶液逐滴加入到溶液1中.

2.2. 分子筛的表征

X-射线粉末衍射(XRD)测试在荷兰帕纳科公司X'pert pro MPD型x射线衍射仪上进行, Cu K_α辐射. 傅里叶变换红外光谱(FT-IR)分析在美国Nicolet MX-1E 560型傅立叶变换红外光谱仪上进行, KBr压片. 紫外-可见漫反射光谱(UV-Vis)光谱分析在TU-1091型光谱仪上进行, BaSO₄作为参比物, 测试范围190~800 nm. 电感耦合等离子体原子发射光谱(ICP-AES)分析在美国Perkin-Elmer公司Optima DV 2000型光谱仪上进行. 在Micromeritics ASAP 2420型气体吸附测试仪上测定样品的比表面积和微孔体积, 以氮气为吸附质. 氨程序升温脱附(NH₃-TPD)在一个连有气相色谱仪(GC 2000II型)的固定床上进行. 将100 mg样品在高纯氩气流(25 ml/min)中673 K下活化1 h, 降至373 K, 然后在此温度下吸附纯氨(20 ml/min) 1.5 h, 再用高纯氩气流(25 ml/min)在此温度下吹扫1 h. 最后, 样品在高纯氩气流(25 ml/min)中以10 K/min的速率从373 K程序升温到873 K.

2.3. 乙烯选择氧化反应

乙烯选择氧化反应在一个500 ml不锈钢高压釜内进

行. 典型的操作如下: 首先, 将4.0 g催化剂、40 ml H₂O₂ (w = 30%)、50 ml蒸馏水和150 ml甲醇装入高压釜, 然后加热至333 K, 通入乙烯, 使反应釜中的压力达到0.7 MPa, 反应8 h. 乙二醇(EG)和乙二醇单甲醚(MME)为主要产物. 反应液中H₂O₂的含量采用碘量法来分析, 产物组成由上海天美科学仪器有限公司GC 7890F型气相色谱仪(SE-54毛细管柱, 15 m × 0.25 mm)分析, 乙腈为内标. 色谱条件如下: 柱箱温度343 K, 汽化室温度493 K, 检测器温度493 K. 催化剂的催化性能评定指标有:

$$X(\text{H}_2\text{O}_2) = [n_0(\text{H}_2\text{O}_2) - n(\text{H}_2\text{O}_2)]/n_0(\text{H}_2\text{O}_2) \times 100\%$$

$$U(\text{H}_2\text{O}_2) = [n(\text{EG}) + n(\text{MME})]/$$

$$[n_0(\text{H}_2\text{O}_2) \times X(\text{H}_2\text{O}_2)] \times 100\%$$

$$S(\text{EG}) = n(\text{EG})/[n(\text{EG}) + n(\text{MME})] \times 100\%$$

$$S(\text{MME}) = n(\text{MME})/[n(\text{EG}) + n(\text{MME})] \times 100\%$$

式中X, U和S分别表示H₂O₂转化率、H₂O₂利用率和EG和MME的选择性; n₀(H₂O₂)和n(H₂O₂)分别表示反应开始和结束时H₂O₂的量; n(EG)和n(MME)分别表示乙二醇和乙二醇单甲醚的量.

3. 结果与讨论

3.1. 双功能钛硅分子筛M-TS-1的表征结果

表1给出了TS-1和M-TS-1催化剂的化学组成和物理特征. 可以明显地看出, TS-1中含有少量的Al. 来源于原料硅溶胶中所含的杂质Al, 并且Al和Ti同时进入了TS-1分子筛的骨架^[16,17]. Al-TS-1, B-TS-1和Fe-TS-1中的Ti和三价元素的含量都比初始凝胶中的含量低. 这表明并不是所有的Ti⁴⁺, Al³⁺, B³⁺和Fe³⁺都参与了晶化过程而进入分子筛的骨架^[5,7,11]. 与TS-1相比, M-TS-1的BET比表面积和微孔体积变化不大, 说明M-TS-1的孔结构保持良好.

图1是TS-1和M-TS-1催化剂的XRD谱. 可以看出, TS-1, Al-TS-1, B-TS-1和Fe-TS-1都具有典型的MFI拓扑结构特征衍射峰, 为分子筛纯相, 说明掺杂Al³⁺, B³⁺或Fe³⁺没有破坏TS-1的结构.

图2是TS-1和M-TS-1催化剂的红外光谱. 可以看出, TS-1, Al-TS-1, B-TS-1和Fe-TS-1在960 cm⁻¹处都有一个明显的吸收峰. 一般认为, 此峰归属于骨架Ti-O-Si的伸缩振动, 说明Ti⁴⁺进入了分子筛的骨架^[18].

图3是TS-1和M-TS-1催化剂的UV-Vis谱. 可以看出, TS-1, Al-TS-1, B-TS-1和Fe-TS-1在220 nm附近都有一个强的吸收峰, 说明分子筛骨架中含有孤立的四配位的钛; 其在270~280 nm附近的弱吸收峰归属于分子筛

中 Ti^{4+} 离子与两个 H_2O 分子配位形成八面体或者部分缩聚的 TiO_x 物种^[19]. TS-1, Al-TS-1, B-TS-1和Fe-TS-1在330 nm附近呈现出一个弱的吸收峰, 说明分子筛中可能含有少量的非骨架锐钛矿型 TiO_2 ^[20]. 这是由于在晶化过程中三价离子与 Ti^{4+} 竞争, 导致一部分 Ti^{4+} 没有进入分子筛的骨架, 而以非骨架的形态存在^[7]. 该结果与表1的元素分析结果一致.

图4是TS-1和M-TS-1催化剂的 NH_3 -TPD谱. 可以看出, TS-1在444.1 K附近有一个明显的 NH_3 脱附峰, 对应的氨气的吸附能力为0.13 mmol/g (见表1). 这表明采用TPABr-NBA体系合成的TS-1具有弱酸性, 主要归因于原料硅溶胶中所携带的微量杂质铝^[16,17]. 掺杂 Al^{3+} , B^{3+} 或 Fe^{3+} 后, 444.1 K附近的氨气脱附峰的强度明显增大. 另外, B-TS-1和Fe-TS-1在677.4 K左右出现一个较弱的氨气脱附峰, 而Al-TS-1则在701.9 K左右出现一个较强的氨气脱附峰. TS-1和M-TS-1酸性强弱的顺序为TS-1 < B-TS-1 < Fe-TS-1 < Al-TS-1 (见表1). 该结果与Trong On等^[7]采用吡啶吸附红外光谱的研究结果基本一致. 以上结果表明, 三价离子的引入增大了TS-1的酸强度和酸量.

Al^{3+} , B^{3+} 或过渡金属离子如 Fe^{3+} 可以在很多矿物中取代硅. 与硅质岩不同的是, 沸石中的同晶取代只能在四配位的晶格点上进行^[6]. 对于Al-TS-1, Fe-TS-1和B-TS-1, 大部分三价离子以四配位的状态嵌入在分子筛的骨架上, 这已经被很多研究者的报道所证实^[5,7-13].

3.2. 双功能钛硅分子筛M-TS-1的催化性能

图5(a)给出了B-TS-1催化乙烯选择氧化的反应结果. 当 $\text{SiO}_2/\text{B}_2\text{O}_3$ 摩尔比从800减小到700时, H_2O_2 基本完全转化, H_2O_2 的利用率及EG和MME的总收率迅速增加, 而EG和MME的选择性变化不大. 当 $\text{SiO}_2/\text{B}_2\text{O}_3$ 摩尔比减小到500时, H_2O_2 的转化率和利用率变化不大, EG和MME的总收率开始降低, 而EG和MME的选择性变化不大. 进一步减小 $\text{SiO}_2/\text{B}_2\text{O}_3$ 摩尔比, H_2O_2 的利用率及EG和MME的总收率迅速降低, 而 H_2O_2 的转化率及EG和MME的选择性变化不大. 这些结果说明, 过量 B^{3+} 的引入会导致 H_2O_2 无效分解程度的增强^[8,9]. 因此, B-TS-1 ($\text{SiO}_2/\text{B}_2\text{O}_3 = 700$)是一个合适的催化剂.

图5(b)给出了Fe-TS-1催化乙烯选择氧化的反应结果. 当 $\text{SiO}_2/\text{Fe}_2\text{O}_3$ 摩尔比从1000减小到720时, H_2O_2 基本完全转化, H_2O_2 的利用率及EG和MME的总收率增加, 而EG和MME的选择性基本不变. 进一步减小 $\text{SiO}_2/\text{Fe}_2\text{O}_3$ 摩尔比, H_2O_2 的转化率变化不大, H_2O_2 的利用

率及EG和MME的总收率开始降低, 而EG和MME的选择性基本不变. 因此, 当 $\text{SiO}_2/\text{Fe}_2\text{O}_3 = 720$ 时催化剂具有相对较好的催化性能.

在乙烯的选择氧化反应中, 采用Al-TS-1 ($\text{Si}/\text{Al} = 252$)为催化剂, 其 H_2O_2 的转化率和利用率分别为98.3%和92.3%, EG和MME的总收率为10.1%. 对比Al-TS-1, B-TS-1和Fe-TS-1的催化性能可以发现, Al-TS-1 ($\text{Si}/\text{Al} = 252$)和B-TS-1 ($\text{Si}/\text{B} = 350$)的催化活性和选择性较高, 其 H_2O_2 利用率达90%以上, 转化率达95%以上, EG和MME的总收率可达10%以上. 而对于Fe-TS-1 ($\text{Si}/\text{Fe} = 360$), EG和MME的总收率只有6.0%, 虽然 H_2O_2 基本完全转化, 但是 H_2O_2 的利用率只有52.1%, 催化选择性较差. 这可能是由于Fe-TS-1具有较强的 H_2O_2 分解能力所致^[5].

3.3. 反应机理

为了研究 H_2O_2 热分解和乙烯选择氧化反应之间的关系, 我们进行了空白实验. 结果表明, H_2O_2 转化率为14.6%, 而 H_2O_2 利用率及EG和MME的总收率都为0. 与上述Al-TS-1, Fe-TS-1和B-TS-1的催化结果对比可知, H_2O_2 的分解和乙烯选择氧化反应之间是竞争关系. 对于Al-TS-1和B-TS-1, H_2O_2 的分解可以忽略, 这与文献^[5,8,9]的报道不一致.

图6(a)是反应时间对Al-TS-1催化乙烯选择氧化反应的影响. 当反应时间从1 h增加到4 h时, H_2O_2 的转化率、 H_2O_2 的利用率及EG和MME的总收率线性增加; 进一步延长反应时间, H_2O_2 的转化率、 H_2O_2 的利用率及EG和MME的总收率变化不大; 整个过程中MME和EG选择性变化不大, 且MME/EG的摩尔比一直保持在2左右. 这是一个很有趣的现象. 因此, 最佳的反应时间为4 h.

图6(b)是反应时间对B-TS-1催化乙烯选择氧化反应的影响. 当反应时间从1 h增加到4 h时, H_2O_2 的转化率、 H_2O_2 的利用率及EG和MME的总收率迅速增加; 继续延长反应时间到7 h, H_2O_2 的转化率、 H_2O_2 的利用率及EG和MME的总收率缓慢增加; 进一步延长反应时间, H_2O_2 的转化率变化不大, 而 H_2O_2 的利用率及EG和MME的总收率开始降低. 整个过程中MME和EG选择性变化不大, 并且MME/EG的摩尔比一直保持在2左右. 这与Al-TS-1上的现象相同. 因此, 最佳的反应时间为7 h. 与Al-TS-1相比, B-TS-1催化乙烯选择氧化的反应时间要长一些, 这可能是由三价离子各自的物理化学性质所决定的^[7].

在乙烯环氧化及后续的开环溶剂解过程中, 如果溶剂解是慢反应, 在产物中应该有环氧乙烷(EO)被检测出

来,但是气相色谱并没有检测出EO.因此,溶剂解是快反应,环氧化反应是慢反应,即决速步骤.由于TS-1具有疏水性,与水相比,甲醇可以很容易地与Ti配位,形成更加稳定的五元环中间体^[21].此外,由于醇的亲核性比水强^[22],EO的开环醇解更加容易进行.因此,在反应过程中MME的选择性一直比EG高.由于生成的EO立即和三价离子所形成的酸性位作用发生开环溶剂解反应,进入TS-1分子筛骨架的三价离子(Al^{3+} 或 B^{3+})应该距离氧化活性位点Ti(IV)很近.基于以上的讨论,我们提出了一个乙烯环氧化及后续开环溶剂解反应生成MME和EG的反应模型(见图式1)^[15].

4. 结论

采用TPABr-NBA合成体系,将三价离子(Al^{3+} , B^{3+}

或 Fe^{3+})和 Ti^{4+} 同时引入到MFI型分子筛的骨架,制备出同时具有氧化和酸催化活性的M-TS-1 ($\text{M} = \text{Al}$, B 或 Fe)分子筛.通过一系列的表征手段对样品进行了系统的表征,结果表明,三价离子进入了分子筛骨架,且M-TS-1依然保持着良好的MFI结构;三价离子的引入提高了TS-1的酸强度和酸量.TS-1和M-TS-1酸性强弱的顺序为 $\text{TS-1} < \text{B-TS-1} < \text{Fe-TS-1} < \text{Al-TS-1}$.通过掺杂不同含量的三价元素来调配其催化氧化和酸催化活性,筛选出合适的双功能钛硅分子筛Al-TS-1 ($\text{Si}/\text{Al} = 252$)和B-TS-1 ($\text{Si}/\text{B} = 350$).二者在乙烯的选择氧化反应中表现出较高的催化性能, H_2O_2 的转化率在95%以上, H_2O_2 的利用率高于90%,EG和MME的总收率可达10%以上,与现有工业上生产EG的收率相当(10%左右).最后,提出了一个M-TS-1催化乙烯环氧化及其后续开环反应的模型.